Engineering Optimization

ISSN: 0305-215X (Print) 1029-0273 (Online) Journal homepage: https://www.tandfonline.com/loi/geno20

Topological optimization for the design of microstructures of isotropic cellular materials

A. Radman, X. Huang & Y.M. Xie

To cite this article: A. Radman, X. Huang & Y.M. Xie (2013) Topological optimization for the design of microstructures of isotropic cellular materials, Engineering Optimization, 45:11, 1331-1348, DOI: 10.1080/0305215X.2012.737781

To link to this article: https://doi.org/10.1080/0305215X.2012.737781

Published online: 03 Dec 2012.

Engineering Optimization, 2013
Vol. 45, No. 11, 1331–1348, http://dx.doi.org/10.1080/0305215X.2012.737781

Taylor & Francis
Taylor & Francis Group

Topological optimization for the design of microstructures of isotropic cellular materials

A. Radman, X. Huang* and Y.M. Xie

School of Civil, Environmental and Chemical Engineering, RMIT University, Melbourne, Australia

(*Received 19 December 2011; final version received 31 August 2012*)

The aim of this study was to design isotropic periodic microstructures of cellular materials using the bidirectional evolutionary structural optimization (BESO) technique. The goal was to determine the optimal distribution of material phase within the periodic base cell. Maximizing bulk modulus or shear modulus was selected as the objective of the material design subject to an isotropy constraint and a volume constraint. The effective properties of the material were found using the homogenization method based on finite element analyses of the base cell. The proposed BESO procedure utilizes the gradient-based sensitivity method to impose the isotropy constraint and gradually evolve the microstructures of cellular materials to an optimum. Numerical examples show the computational efficiency of the approach. A series of new and interesting microstructures of isotropic cellular materials that maximize the bulk or shear modulus have been found and presented. The methodology can be extended to incorporate other material properties of interest such as designing isotropic cellular materials with negative Poisson's ratio.

Keywords: topology optimization; cellular material; bulk modulus; shear modulus; negative Poisson's ratio

1. Introduction

Some natural materials have outstanding mechanical properties and other characteristics as a result of their special microstructures. As an example, honeybee comb is the most studied natural structure that has long fascinated mathematicians, physicists and biologists (Gibson and Ashby 1997; Zhang *et al.* 2010). However, it was not proven until recently that this is the lowest weight structure that can be built with the beeswax to store the largest amount of honey (Mackenzie 1999). These kinds of materials can inspire engineering optimal solutions for design of synthetic materials (Gibson and Ashby 1997).

Material design based on the combination of structural optimization techniques and homogenization theory seeks periodic base cells (microstructures) that enhance the properties of material. In this method, using a structural optimization technique, the topology of material periodic microstructure is optimized with the goal of improving the macromaterial properties. This technique is called 'inverse homogenization' (Bendsøe and Sigmund 2003).

Since the pioneering works of Sigmund (1994, 1995) on periodic truss-like microstructures of materials, various structural optimization techniques have been examined for computationally designing continuum-like microstructures of materials (Neves, Rodrigues, and Guedes 2000; Zhou

*Corresponding author. Email: huang.xiaodong@rmit.edu.au

and Li 2008a, 2008b; Zhou *et al.* 2010). So far, topology optimization methods such as the solid isotropic material with penalization (SIMP) and the level-set have been successfully extended to the design of periodic microstructures of materials or composites (Sigmund 1994, 1995; Neves, Rodrigues, and Guedes 2000; Challis, Roberts, and Wilkins 2008; Zhou and Li 2008a, 2008b; Zhou *et al.* 2010). Recently, (Huang, Radman, and Xie 2011) have extended the bidirectional evolutionary structural optimization (BESO) method for maximizing bulk or shear modulus of cellular materials.

Among various topology optimization algorithms, evolutionary structural optimization (ESO) (Xie and Steven 1993, 1997) was originally developed with the simple concept of gradually removing inefficient elements from the finite element model of the structure so that the resulting topology evolves towards an optimum. A later version of the ESO method, namely BESO (Querin, Steven, and Xie 1998; Yang *et al.* 1999), allows elements to be removed from the least efficient region and added to the most efficient region. Further developments to BESO have been made by theoretically introducing hard-kill BESO (Huang and Xie 2007) and soft-kill BESO (Huang and Xie 2009, 2010a) under certain circumstances. The new BESO method alleviated most of the imperfections of previous versions (Rozvany 2009; Huang and Xie 2010c) and paved the way towards a wider range of engineering applications.

Isotropic materials, in which the properties of materials are invariant with respect to material orientation, are the most common materials used in industry (Barbero 1999) and attractive for engineering applications. For the purpose of designing materials/composites with orthotropic, square symmetric or isotropic elastic tensor, a SIMP scheme is devised to implement the isotropy constraint as a penalty function added to the objective function (Sigmund and Torquato 1997; Sigmund 2000). However, the selection of penalization factors depends on the user's experience and the procedure needs several thousands of iterations to converge owing to the flatness of the modified objective function (Sigmund and Torquato 1997).

Imposing symmetrical constraints on microstructural geometry is another approach to design isotropic materials/composites through inverse homogenization (Neves, Rodrigues, and Guedes 2000; Torquato, Hyun, and Donev 2002). Based on the Neumann principle (Love 1934; Sadd 2005), it is known that in materials made up of periodic base cells (PBCs), the geometric symmetry of the base cell leads to identical symmetry in the constitutive response of the material. To exemplify this idea, Figure 1 shows microstructures of isotropic and anisotropic materials. Figure 1(a) possesses 0°, 60° and 90° symmetries and the resulting material has isotropic elastic properties, whereas such a 60° symmetry does not exist in Figure 1(b) and dissimilar elastic properties are expected along directions 1 and 2. This feature could be used in material design by imposing a geometric constraint on the PBC. However, it should be noted that the symmetry of the microstructure is a sufficient but not necessary condition for the symmetry of material properties (Sigmund and Torquato 1997), and imposing geometric constraints may inhibit the realization of many potential solutions in an inverse homogenization-based optimization.

Recently, the level-set method has been used to design two-phase isotropic composites with maximum stiffness and conductivity (Wilkins, Challis, and Roberts 2007; Challis, Roberts, and Wilkins 2008). In this approach, a 'nearest' isotropic conductivity and elasticity feasible tensor are calculated through the established relationship on effective conductivity and elastic constants of the material. The objective is to minimize the 'distance' between current material properties and calculated 'nearest' isotropic material by modifying the evolution rate in the Hamilton–Jacobi equation. The proposed method is capable of producing microstructures of composites close to conductivity-bulk analytical cross-property bounds (Challis, Roberts, and Wilkins 2008).

This article intends to design the periodic microstructure of isotropic cellular material using the BESO method. It is assumed that the microstructure of cellular material is composed of PBCs. The PBC is discretized into finite elements with periodic boundaries and the homogenization

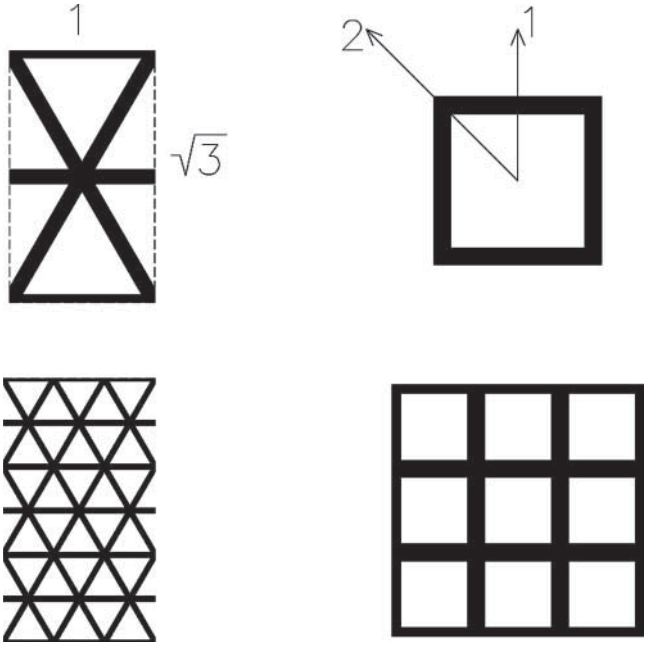

Figure 1. Examples of isotropic and anisotropic microstructures of materials: (a) microstructures of an isotropic material; (b) microstructures of an anisotropic material.

theory is used to calculate the elasticity matrix of the material. Then, the sensitivity analysis is conducted to estimate the effect of individual element on variation in objective and constraints. A Lagrangian multiplier is introduced to make a balance between fulfilment of the objective function and the isotropy constraint. BESO starts from a nearly full solid PBC and gradually removes and adds elements according to the relative ranking of elemental sensitivity numbers until the volume constraint is met and the objective function is convergent. Some two-dimensional (2D) and three-dimensional (3D) examples are presented to demonstrate the effectiveness of the proposed procedure.

2. Isotropy constraint

For the purpose of designing materials with isotropic elastic parameters, the isotropy constraint must be implemented in the optimization algorithm. This section briefly reviews the basic relationships between the elasticity matrix elements and the necessary and sufficient conditions for orthotropic material to be isotropic. The elasticity matrix of a 3D orthotropic material could be expressed as:

$$\mathbf{E} = \begin{bmatrix} E_{11} & E_{12} & E_{13} & 0 & 0 & 0 \\ E_{21} & E_{22} & E_{23} & 0 & 0 & 0 \\ E_{31} & E_{32} & E_{33} & 0 & 0 & 0 \\ 0 & 0 & 0 & E_{44} & 0 & 0 \\ 0 & 0 & 0 & 0 & E_{55} & 0 \\ 0 & 0 & 0 & 0 & 0 & E_{66} \end{bmatrix} \tag{1}$$

Considering the fact that elements of constitutive tensor in isotropic materials should be invariant under any transformation from one coordinate system to another, it can be concluded that relations (2)–(5) are necessary and sufficient conditions for an orthotropic material to be isotropic:

$$E_1 = E_{11} = E_{22} = E_{33} \tag{2}$$

$$E_2 = E_{12} = E_{23} = E_{31} = E_{21} = E_{32} = E_{13} \tag{3}$$

$$E_3 = E_{44} = E_{55} = E_{66} \tag{4}$$

$$E_1 - E_2 = 2E_3 \tag{5}$$

If conditions (2)–(4) hold, then the material is known as cubic symmetric, in which each of the three principal axes has four-fold symmetry. As indicated by Huang, Radman, and Xie(2011), the cubic symmetry conditions of relations (2) to (4) are always met when BESO starts from a cubic symmetric initial guess design and treats all corresponding matrix elements equally. Therefore, in order to obtain an isotropic material, condition (5) needs to be introduced as an additional constraint in the BESO method. By treating cubic symmetric elasticity matrix elements equally, condition (5) can be rewritten as Equation (6a) for 3D cases:

$$C = 2(E_{11} + E_{22} + E_{33}) - (E_{12} + E_{31} + E_{23} + E_{21} + E_{13} + E_{32}) - 4(E_{44} + E_{55} + E_{66}) = 0 \tag{6a}$$

Similarly, condition (5) could be rewritten for 2D plane stress cases as:

$$C = E_{11} + E_{22} - (E_{12} + E_{21}) - 4E_{33} = 0 \tag{6b}$$

It can be shown that Equation (6) is automatically satisfied when the microstructure of a square or cubic symmetric material has additional 60° symmetry. However, as mentioned before, such symmetry in the microstructure is a sufficient but not necessary condition for the isotropic properties of a material (Sigmund and Torquato 1997).

3. Topology optimization problem and sensitivity analysis

Material stiffness could be expressed by its bulk and shear moduli. In the BESO setting, the topology optimization problem of cellular material with a maximum stiffness and with constraints on the isotropy and volume fraction can be expressed as:

$$\text{Maximize} \quad f_1(x) = K \text{ or } G \tag{7a}$$

$$\text{Subject to}: \ C = 0 \tag{7b}$$

$$V^* = \sum_i^n x_i V_i; \ x_i = x_{\min} \text{ or } 1 \tag{7c}$$

$$\mathbf{K_D u}^{mn} = \mathbf{f}^{mn} \tag{7d}$$

where K and G denote the bulk and shear moduli of the material, respectively, $C = 0$ is the isotropy constraint which is defined in Equation (6a) or (6b), V_i is the volume of the ith element, and V^* denotes the prescribed volume of solid phase. Design variable x_i is the density of the ith element, which takes a binary value of either 1 for a solid element or a small value, $x_{\min}$ (*e.g.* 0.001), for a void element. Equation (7d) is the equilibrium equation stated as a finite element problem, in which $\mathbf{K_D}$, $\mathbf{u}^{mn}$ and $\mathbf{f}^{mn}$ are stiffness, periodic displacement and test loads, respectively.

The appropriate expressions for objective functions in terms of invariants of elastic tensor are as follows (Ting 2000; Wilkins, Challis, and Roberts 2007; Challis, Roberts, and Wilkins 2008). The bulk modulus of isotropic materials is:

$$K = \frac{1}{4}E_{iijj},\ i,j \in [1,2] \quad \text{in 2D cases} \tag{8a}$$

$$K = \frac{1}{9}E_{iijj},\ i,j \in [1,3] \quad \text{in 3D cases} \tag{8b}$$

and the shear modulus of isotropic materials is:

$$G = \frac{1}{8}(E_{ijij} + E_{ijji} - E_{iijj}),\ i,j \in [1,2] \quad \text{in 2D cases} \tag{9a}$$

$$G = \frac{1}{20}(E_{ijij} + E_{ijji}) - \frac{1}{30}E_{iijj},\ i,j \in [1,3] \quad \text{in 3D cases} \tag{9b}$$

In the BESO method, the volume constraint can be easily satisfied by gradually removing and adding elements through the evolutionary rate. One of the explored features of the new BESO method is its capability to be integrated with extra constraint in addition to the volume constraint. In the macrostructural optimization with BESO, the stiffness maximization problem has been successfully combined with the volume constraint and with an additional displacement constraint (Huang and Xie 2010b). In this approach, the variation of the displacement is approximately estimated and used to impose the displacement constraint. The topology of the structure is evolved towards the desired solution by introducing a Lagrangian multiplier to adjust the relationship between the objective function and the displacement constraint. This methodology can be extended to impose the isotropy constraint by modifying the original objective function as:

$$f(x) = (1 - |\lambda|) \times f_1(x) + \lambda + C \tag{10}$$

where the Lagrangian multiplier $\lambda \in [-1, 1]$ can be determined by devising a scheme to satisfy the isotropy constraint. It can be seen that the modified objective function is equivalent to the original one when the isotropy constraint is satisfied. The detail about determining the value of λ will be discussed in the following section.

In the BESO method (Huang and Xie 2009, 2010a), the decision making over elements to be solid or void is based on the sensitivity analysis, which estimates the effect of individual elements on the variation in the objective function (or sensitivity numbers). The elastic properties of materials, composed of PBCs with a certain periodic topology, are established through homogenization theory (Bendsøe and Kikuchi 1988; Hassani and Hinton 1998a, 1998b). When the overall dimensions of PBC are very small compared with the sizes of the structural body, the effective elasticity tensor of the macromaterial can be found in terms of the material distribution in the domain of PBC, Ω, as:

$$E^H_{ijkl} = \frac{1}{|Y|}\int_\Omega E_{ijpq}(\bar{\varepsilon}^{kl}_{pq} - \tilde{\varepsilon}^{kl}_{pq})d\Omega \tag{11}$$

where $|\boldsymbol{Y}|$ denotes the volume (or area in 2D) of the PBC domain Ω, and $\bar{\varepsilon}^{kl}_{pq}$ defines the linearly independent unit strain fields. The strain fields $\tilde{\varepsilon}^{kl}_{pq}$ induced by the test strains can be found from the following equation:

$$\int_\Omega E_{ijpq}\varepsilon_{ij}(\upsilon)\tilde{\varepsilon}^{kl}_{pq}d\Omega = \int_\Omega E_{ijpq}\varepsilon_{ij}(\upsilon)\tilde{\varepsilon}^{-kl}_{pq}d\Omega \tag{12}$$

where $\upsilon \in H^1_{per}(\Omega)$ is the Y-periodic admissible displacement field. Equation (12) is the weak form of the standard elasticity equation applied to the PBC under periodic boundary conditions

and is usually solved by finite element analysis of PBC subject to the independent cases of the initial unit strain fields $\bar{\varepsilon}_{pq}^{kl}$. To find elements of homogenized E^H, the base cell is subjected to three or six independent test strain fields in 2D or 3D problems, respectively. For example, in 2D plane stress problems the test strains fields can be selected as $\bar{\varepsilon}_{pq}^{11}(1\ 0\ 0\ 0)^{\mathrm{T}}$, $\bar{\varepsilon}_{pq}^{22} = (0\ 1\ 0\ 0)^{\mathrm{T}}$ and $\bar{\varepsilon}_{pq}^{12} = (0\ 0\ 1\ 0)^{\mathrm{T}}$ or $\bar{\varepsilon}_{pq}^{21} = (0\ 0\ 0\ 1)^{\mathrm{T}}$. For finite element implantation, an equivalent load matrix can be calculated to be used in Equation (7d) (Huang, Radman, and Xie 2011; Bendsøe and Sigmund 2003; Sigmund 1995).

In order to derive the sensitivities of elements with respect to the elasticity properties of the macromaterial, the local material of an element within a PBC can be treated as isotropic and its Young's modulus can be interpolated as the function of the element density as:

$$E(x_i) = E_1 x_i^p \tag{13}$$

where E_I denotes the Young's modulus for a solid element, and p is the penalty exponent. This material model is often called the SIMP model (Rozvany *et al.* 1992; Bendsøe and Sigmund 2003). The penalty exponent $p > 1$ is artificially applied to make sure that the solution indeed converges to a solid/void design. With the help of the above material interpolation scheme, the sensitivity of the homogenized elasticity tensor on the design variable, x_i, can be derived from the adjoint method (Haug, Choi, and Komkov 1986) as:

$$\frac{\partial E_{ijkl}^H}{\partial x_i} = \frac{1}{|Y|}\int_\Omega \frac{\partial E_{pqrs}}{\partial x_i}(\bar{\varepsilon}_{pq}^{kl} - \tilde{\varepsilon}_{pq}^{kl})(\bar{\varepsilon}_{rs}^{ij} - \tilde{\varepsilon}_{rs}^{ij})d\Omega \tag{14}$$

Substituting Equation (13) into Equation (14), the sensitivity of the homogenized elasticity tensor can be rewritten as:

$$\frac{\partial E_{ijkl}^H}{\partial x_i} = \frac{p}{|Y|}\int_\Omega x_i^{p-1} E_{pqrs}^1(\bar{\varepsilon}_{pq}^{kl} - \tilde{\varepsilon}_{pq}^{kl})(\bar{\varepsilon}_{rs}^{ij} - \tilde{\varepsilon}_{rs}^{ij})d\Omega \tag{15}$$

in which E_{pqrs}^1 is the elasticity tensor of the solid material.

The bulk modulus, shear modulus and isotropy constraint could be written in terms of a homogenized constitutive elastic matrix, as shown in Equations (6), (8) and (9). Therefore, the sensitivity numbers of elements can be calculated by:

$$\alpha_i = \frac{df(x)}{dx_i} = (1 - |\lambda|) \times \frac{df_1(x)}{dx_i} + \lambda \times \frac{dC}{dx_i} \tag{16}$$

4. Determination of the Lagrangian multiplier

In the BESO method, since the design variables are restricted to be either $\boldsymbol{x}_{\min}$ or 1, the optimality criterion can be described as sensitivity numbers of solid elements ($\boldsymbol{x}_{\mathrm{i}} = 1$) always being higher than those of void elements ($x_i = x_{\min}$) (Huang and Xie 2010a). Therefore, an update scheme is devised for the design variable x_i by changing from 1 to $x_{\min}$ for elements with the lowest sensitivity numbers and from $x_{\min}$ to 1 for elements with the highest sensitivity numbers. In order to calculate the sensitivity numbers,the value of the Lagrangian multiplier in the objective function as shown in Equation (10) should first be determined.

In general, the Lagrangian multiplier λ should be determined in such a way that the constraint value of C tends to be zero in the next iteration. For this purpose, the following gradient-based

expression is used to estimate the value of the constraint of the next iteration:

$$C^{k+1} \approx C^k + \sum_i \frac{dC^k}{dx_i} \Delta x_i \tag{17}$$

where the superscript k and k+1 denote the current iteration number and the next iteration number, respectively. The derivative of C can be determined numerically by Equations (6) and (15).

At the beginning of each iteration, the sensitivity numbers are calculated by setting $\lambda = 0$. Then, the design variables are updated according to the resulting elemental sensitivity numbers and the given volume constraint. Thus, the value of C^{k+1} is calculated according to Equation (17). If the value of C^{k+1} is positive, then the right-hand summation term of Equation (17) has to be decreased. This could be done by gradually decreasing λ from 0 to -1. The reason for such reduction in λ attributed to the physical meaning of the modified objective function to maximizing the bulk or shear modulus and minimizing the positive C^{k+1} simultaneously. If C^{k+1} is a negative value, then the Lagrangian multiplier has to be gradually increased from 0 to 1. Thus, the modified objective function maximizes the bulk or shear modulus and maximizes the negative C^{k+1} simultaneously.

The accurate value of the Lagrangian multiplier could be found using the bisection algorithm and exploiting two auxiliary variables of λ_{low} and λ_{up} in an internal loop. For instance, at the beginning of internal loops with $\lambda = 0$, if the value of C^{k+1} is positive then the boundary values are set as $\lambda_{low} = -1$, $\lambda_{up} = 0$, and the new value of the Lagrangian multiplier is calculated by setting $\lambda = (\lambda_{up} + \lambda_{low})/2$. Then sensitivity numbers are calculated according to Equation (16), and design variables and C^{k+1} are updated according to the relative ranking of elemental sensitivity numbers. If the updated $C^{k+1} > 0$, the upper bound (λ_{up}) should be replaced with the current λ and the Lagrangian multiplier with $\lambda = (\lambda_{up} + \lambda_{low})/2$. If $C^{k+1} < 0$ then the lower bound (λ_{low}) is replaced with current λ and the Lagrangian multiplier with $\lambda = (\lambda_{up} + \lambda_{low})/2$. The procedure of the internal loop stops when the difference between boundary variables (λ_{low}, λ_{up}) is sufficiently small (*e.g.* 10^{-5}).

5. BESO procedure

To eliminate the numerical instabilities of mesh-dependency and chequerboard patterns in topology optimization, a filtering scheme is used by averaging the elemental sensitivity numbers with the neighbouring element's sensitivity numbers (Huang and Xie 2007, 2010a).The filtering is done using the following weighting equation:

$$\hat{\alpha}_i = \frac{\sum_{j=1}^{N} w_{ij} \alpha_i^1}{\sum_{j=1}^{N} w_{ij}} \tag{18}$$

in which N is the total number of elements in the finite element model and α_i^1 is the left-hand term of Equation (16). The weight factor of w_{ij} is defined as:

$$w_{ij} = \begin{cases} r_{\min} - r_{ij} & \text{if } r_{ij} < r_{\min} \\ 0 & \text{otherwise} \end{cases} \tag{19}$$

in which r_{ij} denotes the distance between element i and element j centres. The filter radius of $r_{\min}$ is to identify the neighbouring elements that affect the sensitivity of element i. To improve the convergence of the solution, elemental sensitivities can be further modified by averaging with their historical information (Huang and Xie 2007).

The whole BESO procedure can be described by the following steps:
Step 1: Define the BESO parameters with prescribed volume (V^*), evolutionary rate (ER), filter radius ($r_{\min}$) and penalty factor (usually $p = 3$).
Step 2: Initiate a finite element of PBC, apply periodic boundary conditions and the test strain field $\bar{\varepsilon}^{kl}_{pq}$. Carry out the finite element analysis to obtain the output strain field of $\tilde{\varepsilon}^{kl}_{pq}$.
Step 3: Calculate $\frac{df_1(x)}{dx_i}$ and $\frac{dC}{dx_i}$ using Equation (15), filter $\frac{df_1(x)}{dx_i}$ and then set $\lambda = 0$.
Step 4: Calculate α_i as per Equation (16). Rank all elemental sensitivity numbers and obtain new set of design variables x_i by applying volume constraint as $V^{k+1} = \max(V^k(1 - ER), V^*)$.
Step 5: Calculate C^{k+1} using Equation (17).
Step 6: If $C^{k+1} > 0$then decrease $\lambda \in [-1, 0]$ using the above-mentioned bisection method; otherwise, increase $\lambda \in [0, 1]$.
Step 7: Repeat Steps 4–6 until the difference between λ_{low} and λ_{up} becomes small enough.
Step 8: Average the sensitivity number with its historical information and then update design variables x_i.
Step 9: Repeat Steps 2–8 until both volume constraint and convergence criterion are met. The convergence criterion is regarded as being satisfied when the changes in the objective function are less than a specific tolerance as

$$error = \frac{\sum_{i=1}^{5}(f_{k-i+1} - f_{k-i-9})}{\sum_{i=1}^{5} f_{k-i+1}} < 0.001 \tag{20}$$

in which f is the defined objective function as shown in Equation (10) and subscript k is the current iteration number.

6. Examples and discussions

In this section, some examples of microstructures that are produced by the proposed method are presented. In all 2D cases, only one-quarter of PBC is modelled because the microstructure loadings and boundary conditions are symmetrical with respect to main perpendicular axes. Similarly, only one-eighth of PBC is modelled in all 3D cases.

The presented results are frequently compared with known analytical bounds of bulk and shear moduli. For well-ordered, quasi-homogeneous and quasi-isotropic composites the upper and lower bounds for bulk and shear moduli have been derived by Hashin and Shtrikman (1963). For cellular materials that are made with a void phase and a solid phase of volume fraction ρ, bulk modulus K and shear modulus G, the Hashin and Shtrikman (HS) upper bounds are given as:

$$K^{up}_{HS} = \frac{\rho KG}{(1-\rho)K + G} \quad \text{2D plane stress bulk modulus upper bound} \tag{21a}$$

$$K^{up}_{HS} = \frac{4KG\rho}{3K(1-\rho) + 4G} \quad \text{3D bulk modulus upper bound} \tag{21b}$$

$$G^{up}_{HS} = \frac{GK\rho}{2(K+G) - \rho(K+2G)} \quad \text{2D plane stress shear modulus upper bound} \tag{22a}$$

$$G^{up}_{HS} = \frac{\rho G(9K + 8G)}{K(15 - 6\rho) + G(20 - 12\rho)} \quad \text{3D shear modulus upper bound} \tag{22b}$$

According to the above relationships the maximum achievable stiffness of cellular materials is always less than that of material made with non-porous solid. It should be pointed out that a

nanoporous material can be made stiffer than its non-porous phase if the pore dimensions are small enough (Duan *et al.* 2006). However, in the present study, the concern is to design conventional cellular materials and it is assumed that the void dimensions are large enough that these nanolevel effects are negligible.

For cubic symmetric materials (also applicable to 2D square symmetric materials), Zener (1948) has proposed an index for the measurement of the anisotropy of materials. This index is frequently used in the literature (Ledbetter and Migliori 2006; Wang *et al.* 2011) and is known as the Zener anisotropy ratio. In terms of three coefficients of cubic symmetric material constitutive matrix, it is defined as:

$$A = \frac{2E_3}{E_1 - E_2} \tag{23}$$

The above ratio defines a measure for resistance to elastic deformation along the [010] direction under a shear stress across the (100) plane with respect to the resistance to deformation along the [110] direction under a shear stress applied across the (110) plane. A comparison with Equation (5) indicates that this ratio should be equal to 1.0 for an isotropic material.

6.1. *2D cellular materials with maximum bulk modulus*

The objective of topology optimization of this example is to obtain materials with maximum bulk modulus. A square finite element model of PBC with dimensions of 120 × 120 is discretized into 120 × 120, four-node quadrilateral elements. Young's modulus and Poisson's ratio of the solid phase are selected as $E = 1$ and $\nu = 0.3$, respectively. The BESO parameters are as follows: the evolutionary rate is ER = 0.006, the filter radius is set equal to $r = 6$ and the prescribed volume (area) of the solid phase is limited to 20% of material volume (area). The initial design is the PBC full of solid elements except for four void elements at the centre.

In order to compare the microstructures with the isotropy constraint and without the isotropy constraint, two microstructures are presented in Figure 2. Figure 2(a) shows the design of the isotropic cellular material while Figure 2(b) shows the design of the square symmetric cellular material without the isotropy constraint. Figure 2(c) and (d) shows the 3 × 3 unit cells of the corresponding microstructures. The corresponding elasticity matrices of the cellular materials are also given in Figure 2. The bulk modulus is 0.0555 for the isotropic cellular material, which shows a good agreement with the HS upper bound, 0.0575. Differing from the isotropic material, the square symmetric material shows non-isotropic properties with a different elasticity matrix in 45°, as given as Figure 2(g).

To indicate the isotropy constraint, Figure 3 shows the variation in the Zener anisotropy ratio for the two cellular materials. It can be seen that the proposed algorithm efficiently sustains the Zener anisotropy ratio close to 1 through the entire process for designing the cellular material with the isotropy constraint. The Zener anisotropy ratio is about 27.5 at the final design stage of square symmetric material without the isotropy constraint.

6.2. *2D cellular materials with maximum shear modulus*

In this example, the objective is to design cellular materials with maximum shear modulus with only 25% of solid phase. The PBCs with dimensions 120 × 120 are discretized into 120 × 120 four-node quadrilateral elements. The BESO parameters used are the evolutionary rate $ER = 0.005$ and filter radius $r_{\min} = 5$. Young's modulus and Poisson's ratio of the solid phase are selected as $E = 1$ and $\nu = 0.3$, respectively. BESO starts from the initial design full of solid elements except for four void elements at the centre.

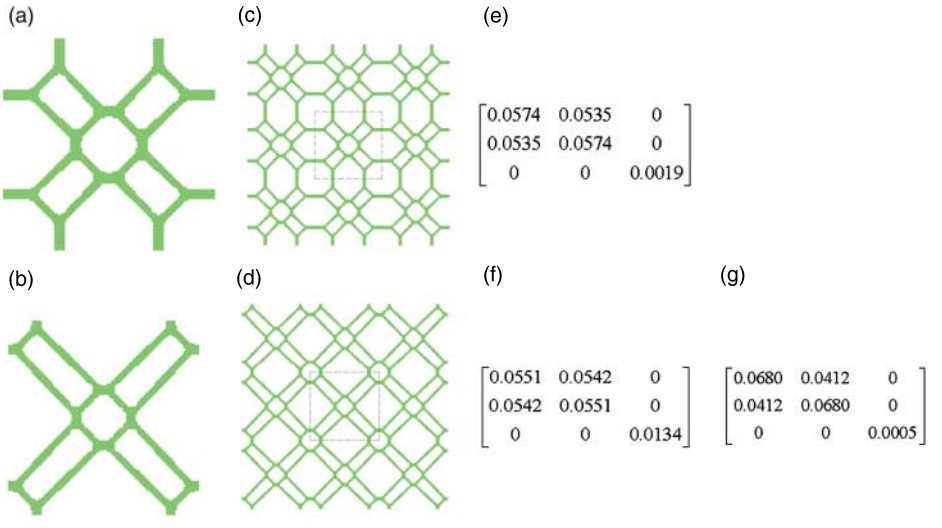

Figure 2. Microstructures of cellular materials with maximum bulk modulus: (a) periodic base cell (PBC) with the isotropy constraint; (b) PBC without the isotropy constraint; (c) 3×3 base cells of (a); (d) 3×3 base cells of (b); (e) elasticity matrix of isotropic material; (f) elasticity matrix of square symmetric material; (g) elasticity matrix of square symmetric material in 45°.

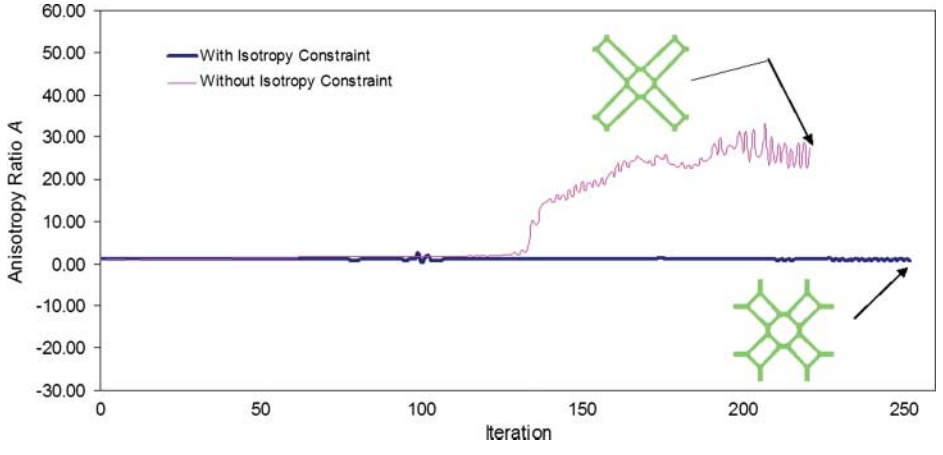

Figure 3. Evolution histories of Zener anisotropy ratio for designing isotropic cellular material and square symmetric cellular material with maximum bulk modulus.

Two microstructures with and without the isotropy constraint are presented in Figure 4. The corresponding 3×3 unit cells and elasticity matrix are also given. The attained shear modulus for the resulting isotropic design is 0.0351, which is very close to the HS shear modulus upper bound, 0.0376. It is also noted that although the objective of this example is to maximize the shear modulus of material, the attained bulk modulus of the isotropic design is 0.0703, which is very close to the HS bulk modulus upper bound (0.0746). Figure 5 shows the evolution history of the Zener anisotropy ratio throughout the whole optimization process. It demonstrates the effectiveness of the proposed algorithm for imposing the isotropy constraint and that the Zener anisotropy ratio is very close to 1 throughout the design process. However, designing the square symmetric material without the isotropy constraint results in $A = 35.3$, as indicated in Figure 5.

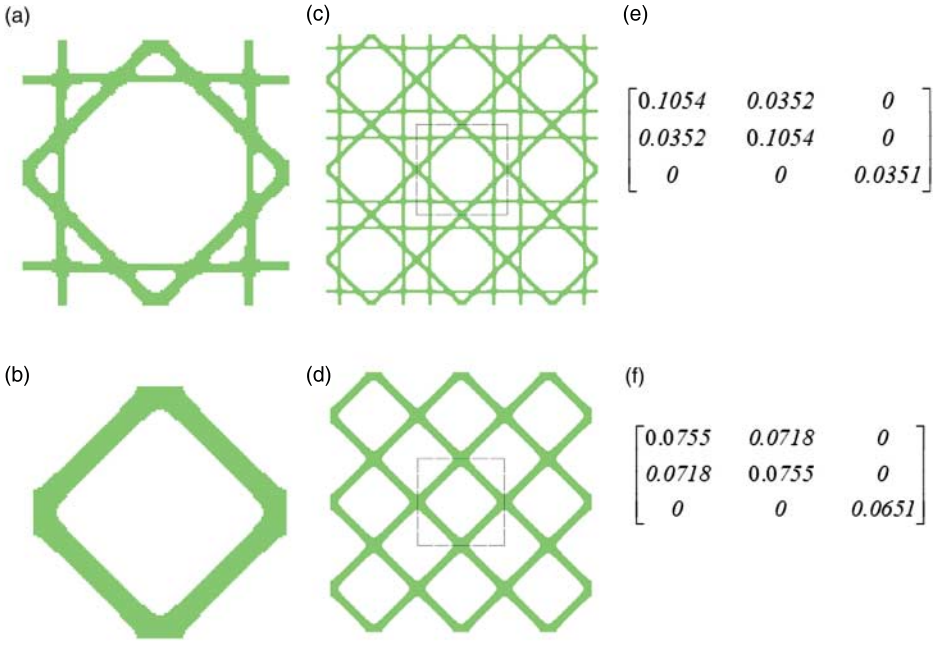

Figure 4. Microstructures of cellular materials with maximum shear modulus: (a) periodic base cell (PBC) with the isotropy constraint; (b) PBC without the isotropy constraint; (c) 3 × 3 base cells of (a); (d) 3 × 3 base cells of (b); (e) elasticity matrix of isotropic material; (f) elasticity matrix of square symmetric material.

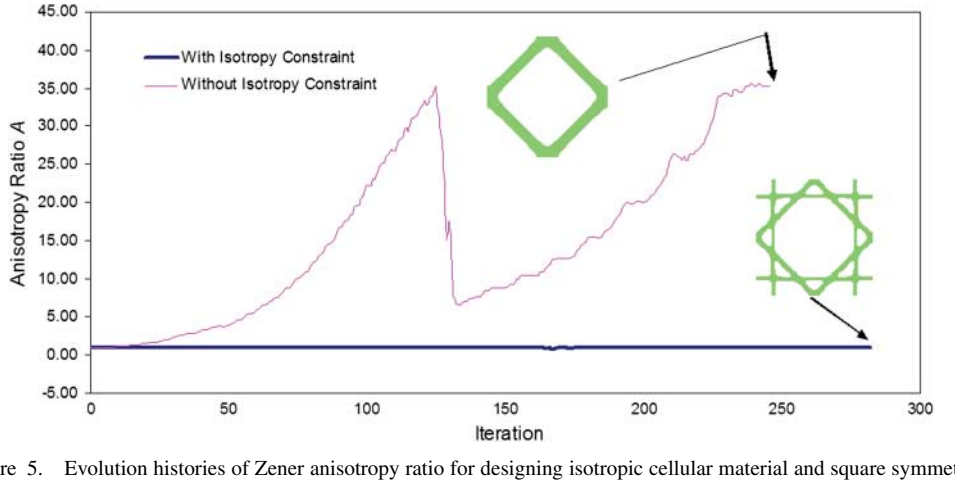

Figure 5. Evolution histories of Zener anisotropy ratio for designing isotropic cellular material and square symmetric cellular material with maximum shear modulus.

6.3. *3D cellular materials with maximum bulk modulus*

The proposed algorithm can be directly applied to 3D cases without any theoretical challenge. The cubic PBC with dimensions 46 × 46 × 46 is discretized into 46 × 46 × 46, eight-node cubic elements and the prescribed solid volume fraction is 20%. BESO parameters are the evolutionary rate $ER = 0.00$ and, filter radius $r_{\min} = 2.5$. Young's modulus and Poisson's ratio of the solid phase are $E = 1$ and $\nu = 0.3$, respectively. The initial design is full of solid elements within the PBC, except for eight void elements at the centre and one void element at eight corners.

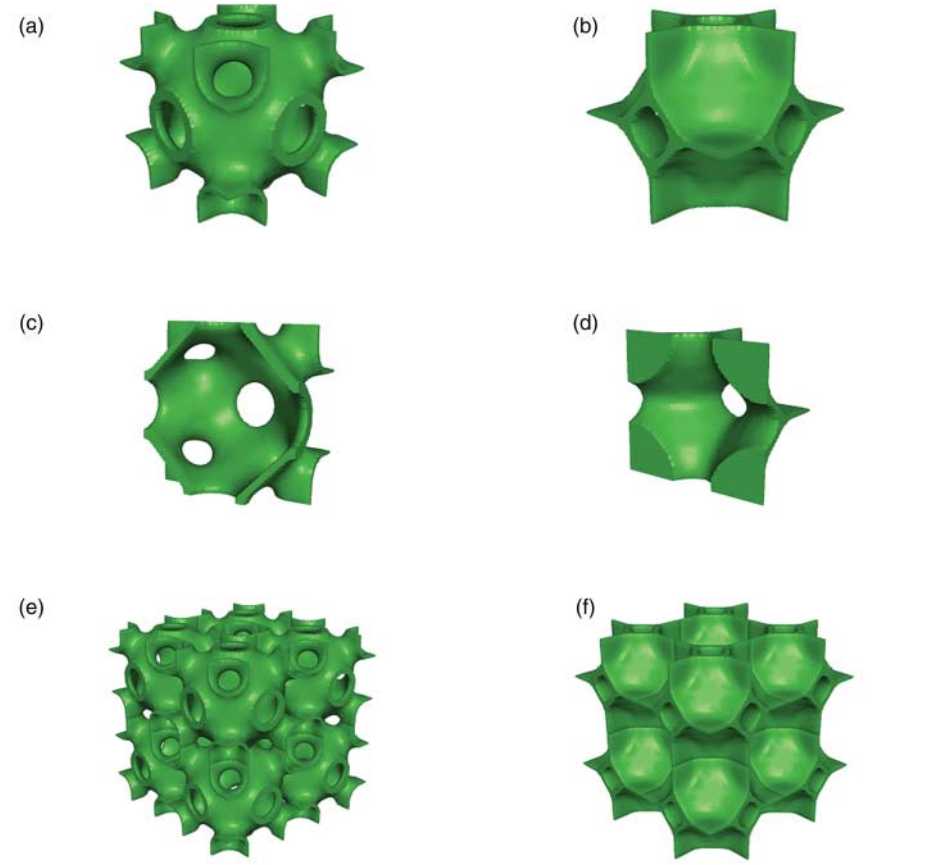

$$\begin{bmatrix} 0.1010 & 0.0393 & 0.0393 & 0 & 0 & 0 \\ & 0.1010 & 0.0393 & 0 & 0 & 0 \\ & & 0.1010 & 0 & 0 & 0 \\ & & & 0.0308 & 0 & 0 \\ & sym & & & 0.0308 & 0 \\ & & & & & 0.308 \end{bmatrix} \quad \begin{bmatrix} 0.0975 & 0.0534 & 0.0534 & 0 & 0 & 0 \\ & 0.0975 & 0.0534 & 0 & 0 & 0 \\ & & 0.0975 & 0 & 0 & 0 \\ & & & 0.0386 & 0 & 0 \\ & sym & & & 0.0386 & 0 \\ & & & & & 0.0386 \end{bmatrix}$$

Figure 6. Three-dimensional microstructures of materials with maximum bulk modulus: (a) periodic base cell (PBC) with isotropy constraint; (b) PBC without isotropy constraint; (c) half of the PBC shown in (a); (d) half of the PBC shown in (b); (e) 2×2 base cells of (a); (f) 2×2 base cells of (b); (g) isotropic material elasticity matrix; (h) cubic symmetric material elasticity matrix.

Figure 6(a) and (b) shows two microstructures that are designed for the maximum bulk modulus with and without isotropy constraints, respectively. In order to show the interior microstructure, only half of the base cells are shown in Figure 6(c) and (d). The corresponding 2×2 unit cells and elasticity matrix are also shown in Figures 6. The bulk modulus of cellular material with the isotropy constraint is 0.0599. Figure 7 shows the evolution history of the Zener anisotropy ratio throughout iterations for both designs and indicates that the Zener anisotropy ratio is very close to 1 for the design with the isotropy constraint.

When BESO starts from the initial design which is full of solid elements except for eight void elements at the centre, and BESO parameters are set as $ER = 0.007$ and $r_{\min} = 3$, the resulting topologies of Figure 8 are obtained. The bulk modulus of the resulting isotropic cellular material

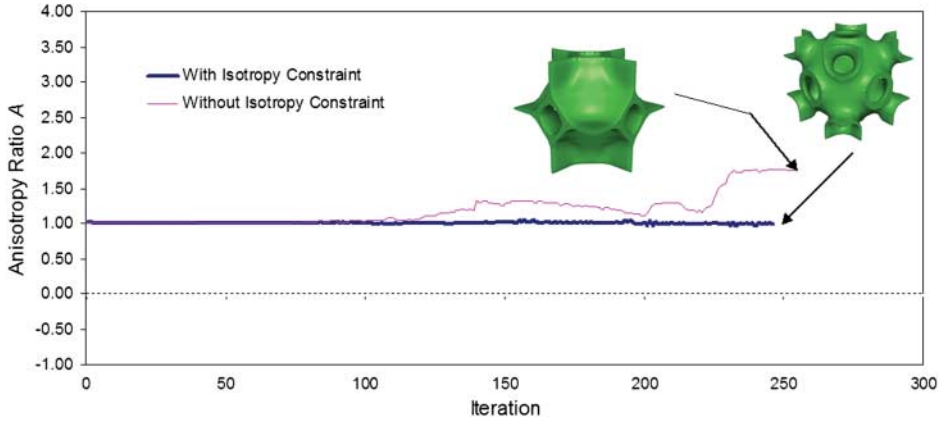

Figure 7. Evolution histories of Zener anisotropy ratio for designing isotropic cellular material and cubic symmetric cellular material with maximum bulk modulus.

is 0.0585 and the Zener anisotropy ratio is $A = 1.0$. The Zener anisotropy ratio of the resulting cubic symmetric cellular material is 2.52 and its corresponding bulk modulus is equal to 0.0619.

6.4. *3D cellular materials with maximum shear modulus*

The objective of this example is to design 3D microstructures of cellular materials with maximum shear modulus. The PBC with dimensions $60 \times 60 \times 60$ is discretized with $60 \times 60 \times 60$, eight-node cubic finite elements. Young's modulus and Poisson's ratio of the solid phase are selected as $E = 1$ and $\nu = 0.3$, respectively. The BESO parameters are evolution rate $ER = 0.007$ and filter radius $r_{\min} = 3$. BESO starts from the initial design, which is full of solid elements within PBC, except for eight void elements at the centre of the design domain and four void elements at the centre of each of the six sides of the model. The prescribed volume fraction of the solid phase is 40%.

Figure 9 shows the resulting microstructures and elasticity matrices of isotropic cellular material and cubic symmetric cellular material. The shear modulus of the isotropic cellular material is equal to 0.0984, which is very close to the HS shear modulus upper bound, 0.0995. The Zener anisotropy ratio for the isotropic cellular material is $A = 1.0$. However, the topology optimization without the isotropy constraint results in a microstructure with a Zener anisotropy ratio of 1.25. It is noticed that the bulk modulus of isotropic material (0.1405) is also very close to the HS upper bound (0.1688), although the objective of this example is to maximize the shear modulus.

6.5. *2D isotropic cellular materials with negative Poisson's ratio*

To demonstrate the effectiveness of the proposed procedure in imposing the isotropy constraint for other objective function, the below examples seek 2D isotropic cellular materials with negative Poisson's ratio.

Negative Poisson's ratio in foams has been observed by Lakes (1987) and it has been further demonstrated qualitatively (Phan-Thien and Karihaloo 1994) that a composite material with randomly distributed microstructures can have isotropic behaviour with negative Poisson's ratio. The key feature of their microstructures is the existence of re-entrant corners, which has been already noticed (Lakes 1987).

Through inverse homogenization, Sigmund (1994) found that designing of cellular composites with negative Poisson's ratio from continuum-like materials is very difficult. The negative value

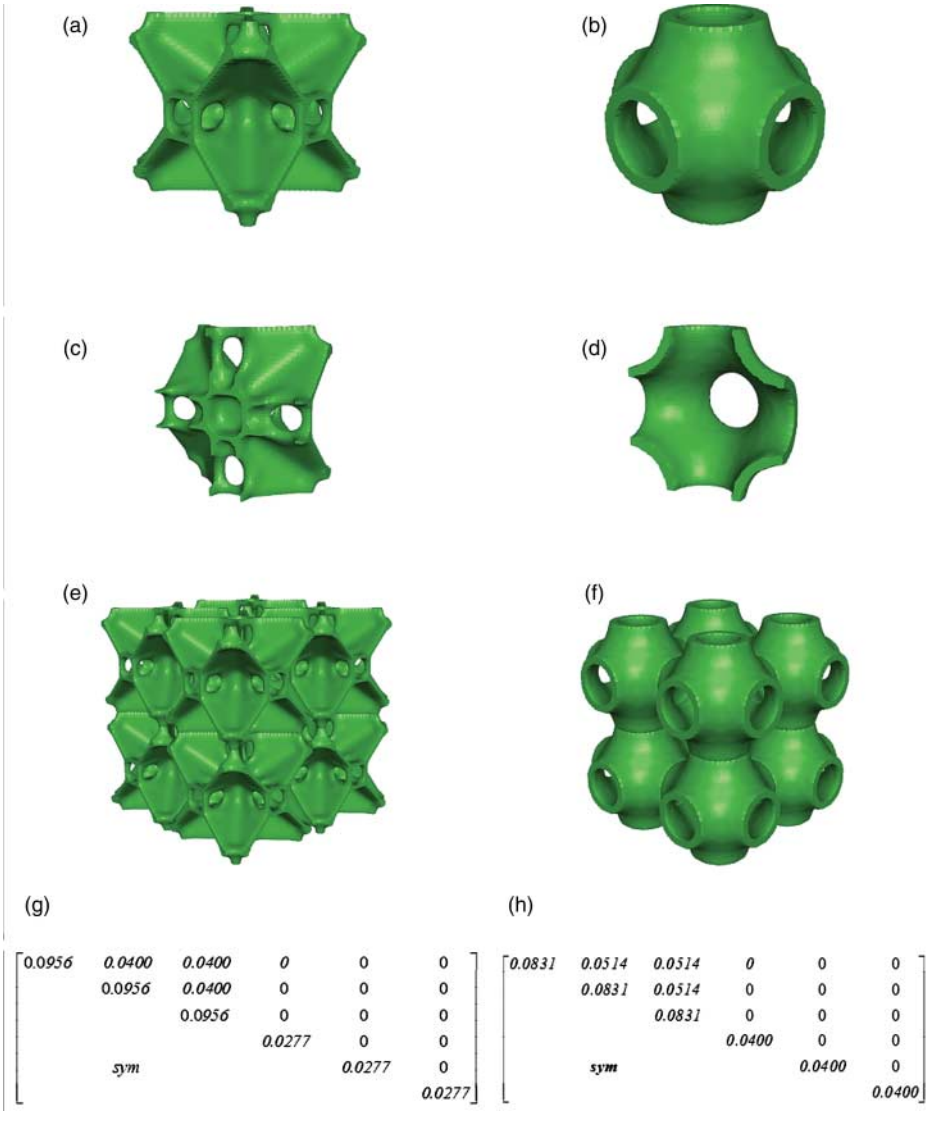

$$\begin{bmatrix} 0.0956 & 0.0400 & 0.0400 & 0 & 0 & 0 \\ & 0.0956 & 0.0400 & 0 & 0 & 0 \\ & & 0.0956 & 0 & 0 & 0 \\ & & & 0.0277 & 0 & 0 \\ & sym & & & 0.0277 & 0 \\ & & & & & 0.0277 \end{bmatrix} \quad \begin{bmatrix} 0.0831 & 0.0514 & 0.0514 & 0 & 0 & 0 \\ & 0.0831 & 0.0514 & 0 & 0 & 0 \\ & & 0.0831 & 0 & 0 & 0 \\ & & & 0.0400 & 0 & 0 \\ & sym & & & 0.0400 & 0 \\ & & & & & 0.0400 \end{bmatrix}$$

Figure 8. Three-dimensional microstructures of materials with maximum bulk modulus: (a) periodic base cell (PBC) with the isotropy constraint; (b) PBC without the isotropy constraint; (c) half of the PBC shown in (a); (d) half of the PBC shown in (b); (e) 2×2 base cells of (a); (f) 2×2 base cells of (b); (g) isotropic material elasticity matrix; (h) cubic symmetric material elasticity matrix.

of Poisson's ratio can reach -1 when the shear modulus of material is much larger than its bulk modulus. The numerical experiences indicate that the attainable values of E_{12} and E_{33} are connected (Sigmund 1994). Here, the following statement is used as the objective function to find a material with negative Poisson's ratio:

$$\text{Minimize } f_1(x) = E_{21} + E_{12} - 2E_{33} \tag{24}$$

In 2D examples, the PBC with dimensions 160×160 is discretized into 160×160 four-node quadrilateral elements. The prescribed volume (area) fraction of the solid phase is 35% of the total volume (area). Young's modulus and Poisson's ratio of the solid phase are $E = 1$ and $\nu = 0.2$,

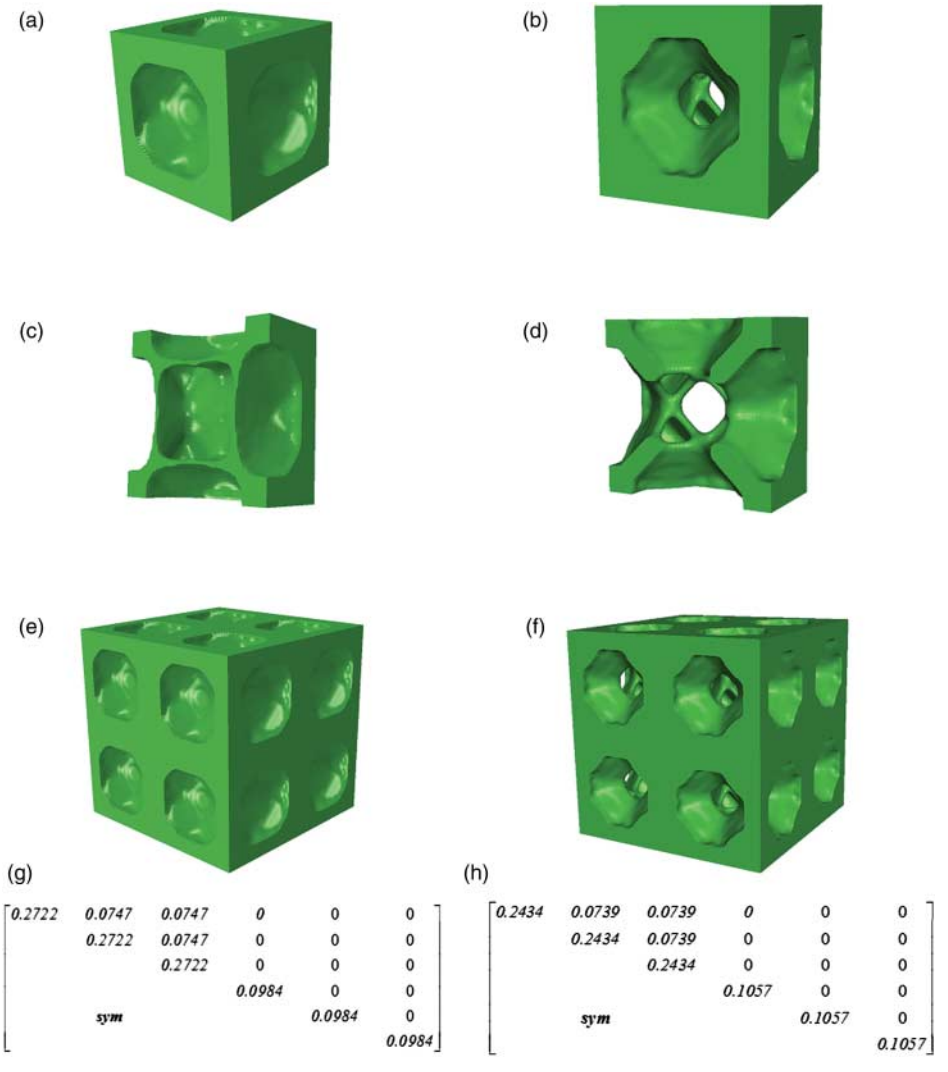

$$\begin{bmatrix} 0.2722 & 0.0747 & 0.0747 & 0 & 0 & 0 \\ & 0.2722 & 0.0747 & 0 & 0 & 0 \\ & & 0.2722 & 0 & 0 & 0 \\ & & & 0.0984 & 0 & 0 \\ & sym & & & 0.0984 & 0 \\ & & & & & 0.0984 \end{bmatrix} \qquad \begin{bmatrix} 0.2434 & 0.0739 & 0.0739 & 0 & 0 & 0 \\ & 0.2434 & 0.0739 & 0 & 0 & 0 \\ & & 0.2434 & 0 & 0 & 0 \\ & & & 0.1057 & 0 & 0 \\ & sym & & & 0.1057 & 0 \\ & & & & & 0.1057 \end{bmatrix}$$

Figure 9. Three-dimensional microstructures of materials with maximum shear modulus: (a) periodic base cell (PBC) with the isotropy constraint; (b) PBC without the isotropy constraint; (c) half of the PBC shown in (a); (d) half of the PBC shown in (b); (e) 2×2 base cells of (a); (f) 2×2 base cells of (b); (g) isotropic material elasticity matrix; (h) cubic symmetric material elasticity matrix.

respectively. The BESO parameters are $ER = 0.004$ and $r_{\min} = 4$. BESO starts from the initial finite element model, which is full of solid elements except for four void elements at the centre. Figure 10 illustrates the resulting microstructure of the isotropic cellular material with a negative Poisson's ratio, -0.5482. When a smaller filter radius $r_{\min} = 1.5$ is used and the volume fraction is set to be 30%, a different microstructure is obtained, as shown in Figure 11. According to its elasticity matrix, Poisson's ratio of the resulting isotropic cellular material is -0.4118 and the Zener anisotropy ratio is very close to 1. One can easily perceive the lateral expansion of the microstructures in Figures 10 and 11 when they are under tensile force owing to existence of the re-entrant corners. These microstructures are similar to the qualitative models in Phan-Thien and Karihaloo (1994).

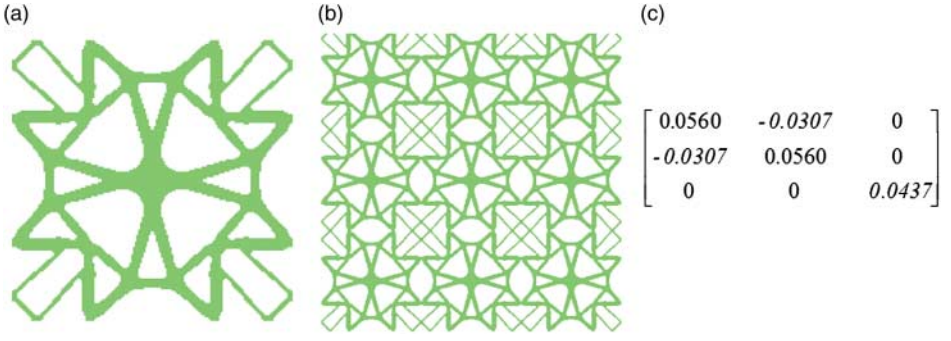

Figure 10. Microstructure of isotropic material with negative Poisson's ratio: (a) periodic base cell; (b) 3 × 3 unit cells; (c) isotropic material elasticity matrix.

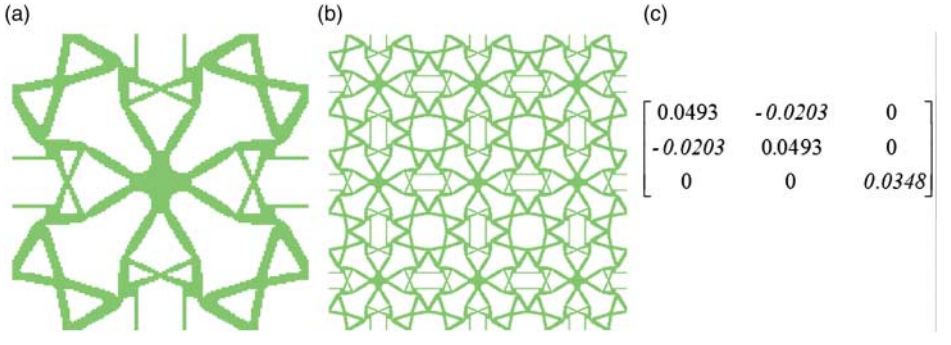

Figure 11. Microstructure of isotropic material with negative Poisson's ratio: (a) periodic base cell; (b) 3 × 3 unit cells; (c) isotropic material elasticity matrix.

7. Conclusion

This article proposes a new approach for designing isotropic cellular materials with maximum bulk modulus or maximum shear modulus using the BESO method. The isotropy of the materials is considered as an additional constraint to the optimization problem. The modified objective is constructed by introducing a Lagrange multiplier to implement the isotropy constraint. With the established elemental sensitivity numbers, the PBC gradually evolves to an isotropic microstructure with the specified material properties. The effectiveness of the proposed procedure has been demonstrated by topology optimization of microstructures of isotropic cellular materials with maximum bulk modulus or maximum shear modulus. Examples clearly show the difference between designing square (cubic) symmetric cellular materials without the isotropy constraint and isotropic cellular materials with the isotropy constraint. The evolution histories of the Zener anisotropy ratio indicate that the isotropy constraint has been properly incorporated into the optimization algorithm for designing all isotropic material cases. The given examples also demonstrate that the proposed method can be extended to designing isotropic cellular materials with other specific properties such as negative Poisson's ratio.

Acknowledgements

This research is supported by the Australian Research Council under its Discovery Projects funding scheme (project number DP1094403).

References

Barbero, E. J. 1999. *Introduction to Composite Materials Design*. London: Taylor & Francis.

Bendsøe, M. P., and N. Kikuchi. 1988. "Generating Optimal Topologies in Optimal Design Using a Homogenization Method." *Computer Methods in Applied Mechanics and Engineering*, 71, 197–224.

Bendsøe, M. P., and O. Sigmund. 2003. *Topology Optimization: Theory, Methods and Application.* Berlin: Springer.

Challis, V. J., A. P. Roberts, and A. H. Wilkins. 2008. "Design of Three Dimensional Isotropic Microstructures for Maximized Stiffness and Conductivity." *International Journal of Solids and Structures*, 45, 4130–4146.

Duan, H. L., J. Wang, B. L. Karihaloo, and Z. P. Huang. 2006. "Nanoporous Materials Can be Made Stiffer than Non-Porous Counterparts by Surface Modification." *Acta Materialia*, 54, 2983–2990.

Gibson, L. J., and M. F. Ashby. 1997. *Cellular Solids: Structures and Properties*. Cambridge: Cambridge University Press.

Hashin, Z., and S. Shtrikman. 1963. "A Variational Approach to the Theory of the Elastic Behaviour of Multiphase Materials." *Mechanics and Physics of Solids*, 11, 120–141.

Hassani, B., and E. Hinton. 1998a. "A Review of Homogenization and Topology Optimization I—Homogenization for Media with Periodic Structure." *Computers and Structures*, 69, 707–717.

Hassani, B., and E. Hinton. 1998b. "A Review of Homogenization and Topology Optimization II—Analytical and Numerical Solution of Homogenization Equations." *Computers and Structures*, 69, 719–738.

Haug, E. J., K. K. Choi, and V. Komkov. 1986. *Design Sensitivity Analysis of Structural Systems*. Orlando, FL: Academic Press.

Huang, X., A. Radman, and Y. M. Xie. 2011. "Topological Design of Microstructures of Cellular Materials for Maximum Bulk or Shear Modulus." *Computational Materials Science*, 50, 1861–1870.

Huang, X., and Y. M. Xie. 2007. "Convergent and Mesh-Independent Solutions for the Bi-Directional Evolutionary Structural Optimization Method." *Finite Elements in Analysis and Design*, 43, 1039–1049.

Huang, X., and Y. M. Xie. 2009. "Bi-Directional Evolutionary Topology Optimization of Continuum Structures with One or Multiple Materials." *Computational Mechanics*, 43, 393–401.

Huang, X., and Y. M. Xie. 2010a. *Evolutionary Topology Optimization of Continuum Structures: Methods and Applications*. Chichester: John Wiley & Sons.

Huang, X., and Y. M. Xie. 2010b. "Evolutionary Topology Optimization of Continuum Structures with an Additional Displacement Constraint." *Structural and Multidisciplinary Optimization*, 40, 409–416.

Huang, X., and Y. M. Xie. 2010c. "A Further Review of ESO Type Methods for Topology Optimization." *Structural and Multidisciplinary Optimization*, 41, 671–683.

Lakes, R. 1987. "Foam Structures with a Negative Poisson's Ratio." *Science*, 235, 1038–1040.

Ledbetter, H., and A. Migliori. 2006. "A General Elastic-Anisotropy Measure." *Journal of Applied Physics*, 100, 063516.

Love, A. 1934. *A Treatise of the Mathematical Theory of Elasticity.* London: Cambridge University Press.

Mackenzie, D. 1999. "Proving the Perfection of the Honeycomb." *Science*, 285, 1338–1339.

Neves, M. M., H. Rodrigues, and J. M. Guedes. 2000. "Optimal Design of Periodic Linear Elastic Microstructures." *Computers and Structures*, 76, 421–429.

Phan-Thien, N., and B. L. Karihaloo. 1994. "Materials with Negative Poisson's Ratio: A Qualitative Microstructural Model." *Journal of Applied Mechanics*, 61, 1001–1004.

Querin, O. M., G. P. Steven, and Y. M. Xie. 1998. "Evolutionary Structural Optimization (ESO) Using a Bi-Directional Algorithm." *Engineering Computations*, 15, 1031–1048.

Rozvany, G. 2009. "A Critical Review of Established Methods of Structural Topology Optimization." *Structural and Multidisciplinary Optimization*, 37, 217–237.

Rozvany, G. I. N., M. Zhou, and T. Birker. 1992. "Generalized Shape Optimization without Homogenization." *Structural and Multidisciplinary Optimization*, 4, 250–252.

Sadd, M. H. 2005. *Elasticity Theory, Application and Numerics*. New York: Elsevier.

Sigmund, O. 1994. "Materials with Prescribed Constitutive Parameters: An Inverse Homogenization Problem." *International Journal of Solids and Structures*, 31, 2313–2329.

Sigmund, O. 1995. "Tailoring Materials with Prescribed Elastic Properties." *Mechanics of Materials*, 20, 351–368.

Sigmund, O. 2000. "A New Class of Extremal Composites." *Journal of the Mechanics and Physics of Solids*, 48, 397–428.

Sigmund, O., and S. Torquato. 1997. "Design of Materials with Extreme Thermal Expansion Using a Three-Phase Topology Optimization Method." *Mechanics and Physics of Solids*, 45, 1037–1067.

Ting, T. C. T. 2000. "Anisotropic Elastic Constants that are Structurally Invariant." *Quarterly Journal of Mechanics and Applied Mathematics*, 53, 511–523.

Torquato, S., S. Hyun, and A. Donev. 2002. "Multifunctional Composites: Optimizing Microstructures for Simultaneous Transport of Heat and Electricity." *Physical Review Letters*, 89, 266601.

Wang, L., J. Lau, E. L.Thomas, and M. C. Boyce. 2011. "Co-Continuous Composite Materials for Stiffness, Strength, and Energy Dissipation." *Advanced Materials*, 23, 1524–1529.

Wilkins, A. H., C. J. Challis, and A. P. Roberts. 2007. "Isotropic, Stiff, Conducting Structures via Topology Optimization." 7th World Congress on Structural and Multidisciplinary Optimization, Seoul, Korea.

Xie, Y. M., and G. P. Steven. 1993. "A Simple Evolutionary Procedure for Structural Optimization." *Computers and Structures*, 49, 885–896.

Xie, Y. M., and G. P. Steven. 1997. *Evolutionary Structural Optimization.* London: Springer.

Yang, X.Y., Y. M. Xie, G. P. Steven, and O. M. Querin. 1999. "Bidirectional Evolutionary Method for Stiffness Optimization." *AIAA Journal*, 37,1483–1488.

Zener, C. 1948. *Elasticity and Anelasticity of Metals*. Chicago: University of Chicago Press.
Zhang, K., H. Duan, B. L. Karihaloo, and W. Jianxiang. 2010. "Hierarchical, Multilayered Cell Walls Reinforced by Recycled Silk Cocoons Enhance the Structural Integrity of Honeybee Combs." *Proceedings of the National Academy of Sciences of the USA*, 107, 9502–9506.
Zhou, S., and Q. Li. 2008a. "Design of Graded Two-Phase Microstructures for Tailored Elasticity Gradients." *Journal of Materials Science*, 43, 5157–5167.
Zhou, S., and Q. Li. 2008b. "Computational Design of Multi-Phase Microstructural Materials for Extremal Conductivity." *Computational Materials Science*, 43, 549–564.
Zhou, S., W. Li, G.Sun, and Q. Li. 2010. "A Level-Set Procedure for the Design of Electromagnetic Metamaterials." *Optics Express*, 18, 6693–6702.